JACS JOURNAL OF THE AMERICAN CHEMICAL SOCIETY
COMMUNICATION
pubs.acs.org/JACS

Spatial Nonuniformity in Resistive-Switching Memory Effects of NiO

Keisuke Oka,[†] Takeshi Yanagida,[*,†,‡] Kazuki Nagashima,[†] Masaki Kanai,[†] Tomoji Kawai,[*,†,§] Jin-Soo Kim,[§] and Bae Ho Park[§]

[†]Institute of Scientific and Industrial Research, Osaka University, 8-1 Mihogaoka Ibaraki, Osaka 567-0047, Japan

[‡]PRESTO, Japan Science and Technology Agency, 4-1-8 Honcho Kawaguchi, Saitama 332-0012, Japan

[§]Division of Quantum Phases and Devices, Department of Physics, Konkuk University, Seoul 143-701, Korea

S *Supporting Information*

ABSTRACT: Electrically driven resistance change phenomenon in metal/NiO/metal junctions, so-called resistive switching (RS), is a candidate for next-generation universal nonvolatile memories. However, the knowledge as to RS mechanisms is unfortunately far from comprehensive, especially the spatial switching location, which is crucial information to design reliable devices. In this communication, we demonstrate the identification of the spatial switching location of bipolar RS by introducing asymmetrically passivated planar NiO nanowire junctions. We have successfully identified that the bipolar RS in NiO occurs near the cathode rather than the anode. This trend can be interpreted in terms of an electrochemical redox model based on ion migration and p-type conduction.

Resistance-based nonvolatile memory effects in metal—oxide—metal capacitors, frequently called "Memristor"[1] and/or "ReRAM",[2] have attracted much attention due to the potentials toward ultimate universal nonvolatile memory[3] and also artificial neural computing.[1] NiO has been particularly considered to be one of the most promising materials for such novel devices. However, progress has been delayed by difficulties in understanding the exact mechanisms of memory effects,[4] including the spatial conductive distribution of resistive switching (RS), which are crucial for creating and designing reliable RS devices because the resistive switching location is considered to be a heat source during operations. Unfortunately, conventional capacitor-type RS devices cannot provide such spatial information within the switching layer. A planar-type nanowire RS junction offers a nanoscale platform to investigate such internal spatial distribution of RS, which in principle cannot be revealed by conventional capacitor-type structures. Previously, we have demonstrated the feasibility and reliability of such planar-type NiO nanowire RS junctions.[5−8] The RS properties in such planar-type RS devices were found to be essentially comparable to the capacitor-type RS devices in terms of the switching electric field, i.e. the differences are the junction structure and the surroundings. Utilizing intentionally the features of planar-type RS junctions allows us to extract directly the spatial RS information, which had not been available. Here we report the spatial location of the resistance switching in NiO by introducing intentionally the asymmetric passivation layer in the planar-type NiO nanowire junctions. Compared with previous works,[7] the major advancement in this study is the use of asymmetrically passivated structures, which essentially allows us to identify directly the switching location of RS.

Four types of Pt/NiO nanowire/Pt RS junctions were fabricated by varying the spatial location of amorphous SiO_2 passivation layer on the junctions. (See Figure 1.) In Type I, only the anode side is passivated, whereas the cathode side is only passivated for Type II. Type III is totally not passivated, and Type IV is entirely passivated. Comparing these four types of junctions allows us to identify the switching location of RS since the presence of the passivation layer affects the RS events. These junctions were constructed on n-type Si substrate capped with a 300 nm SiO_2 layer by a combined process of electron beam (EB) lithography, RF sputtering, and pulse-laser deposition (PLD) techniques (see the details in SI). The fabricated NiO nanowires with 100 nm size were polycrystalline form. (See the structural data in SI.) We defined the position of Pt electrodes (70 nm thickness) with the nanowire by EB lithography. The gap spacing of fabricated electrodes was typically 500 nm for Types I and II junctions and 300 nm for Types III and IV junctions. Amorphous SiO_2 passivation layer with 50 nm thickness was deposited onto the junctions by controlling the position for each device. FESEM (HITACHI S-4300) and TEM (JEOL JEM-3000F) were used to characterize the fabricated junctions. Current—voltage ($I-V$) measurements of junctions were performed by using a semiconductor analyzer (Keithley 4200SCS) in DC sweep mode (see the details in SI).

Figure 1 shows the schematics, FESEM and TEM-ED images of fabricated junctions of four types (see the details of structures in SI). $I-V$ data of the four junctions are shown in Figure 2. The transport measurements were performed with the compliance current of 10^{-9} A. All junctions consistently exhibited a polarity-dependent RS. After a so-called forming process (details in SI), which is defined as the initial process to introduce the electrical conduction within pristine insulative matrix by high electric field, the devices exhibited the $I-V$ curves in Figure 2. Note that the pristine resistance prior to the forming process was almost the same value in all junctions. Hereafter, the positively biased electrode during the forming process is defined as 'anode', while the grounded electrode is defined as 'cathode'. When applying the positive electric field, the junction resistance tended to decrease (SET process), whereas applying the negative electric field

Received: July 7, 2011
Published: July 21, 2011

ACS Publications © 2011 American Chemical Society

dx.doi.org/10.1021/ja206063m | *J. Am. Chem. Soc.* 2011, 133, 12482–12485

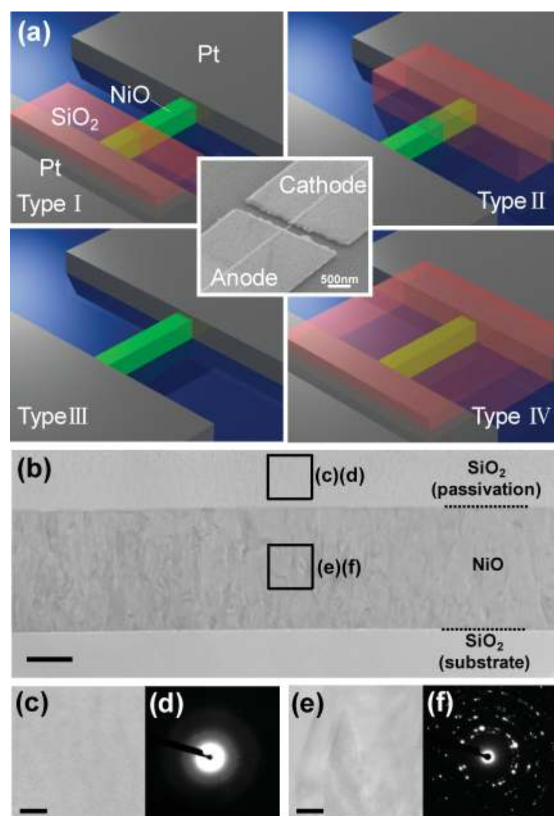

Figure 1. (a) Various Pt/NiO/Pt nanowire junctions. Type I (amorphous SiO_2 passivation layer only for anode side), Type II (amorphous SiO_2 passivation layer only for cathode side), Type III (without passivation layer), and Type IV (amorphous SiO_2 passivation layer for entire region). Middle image shows typical FESEM image of fabricated junction. (b) Low-magnification cross-sectional HRTEM image of fabricated NiO nanowire junction. Scale bar is 50 nm. (c) High-magnification HRTEM image of amorphous SiO_2 passivation layer. Scale bar is 10 nm. (d) Selected area electron diffraction (SAED) pattern of SiO_2 passivation. (e) High-magnification HRTEM image of NiO layer. Scale bar is 10 nm. (f) Selected area electron diffraction (SAED) pattern of SiO_2 passivation.

resulted in the increase of junction resistance (RESET process). The two resistance states (low-resistance state: LRS, high-resistance state: HRS) were kept constant as long as the electric field was applied with the same polarity. The memory retention time was confirmed at least up to 10^4 s. (See the retention data in SI.) Thus, the observed RS in all junctions was consistently a polarity dependent "bipolar" nonvolatile memory effect.[9,10] More importantly the shape of $I-V$ data was found to strongly depend on the spatial configurations of SiO_2 passivation layer. Type I junction with the passivation layer near the anode showed $I-V$ data similar to that of Type III without the passivation layer. On the other hand, $I-V$ data of Type II with the passivation layer near the cathode was very similar to that of Type IV with the passivation layer for entire region. Table 1 shows the quantitative comparisons between the four junctions in terms of the ratio of SET and RESET voltages. Here we define the SET voltage as the applied voltage when the current reaches the compliance current of 10^{-9} A, and the RESET voltage as the voltage when the junction resistance shows the minimum. In the two similarities between junctions, the common feature is clearly the presence or the absence of the passivation layer near the cathode. In other words,

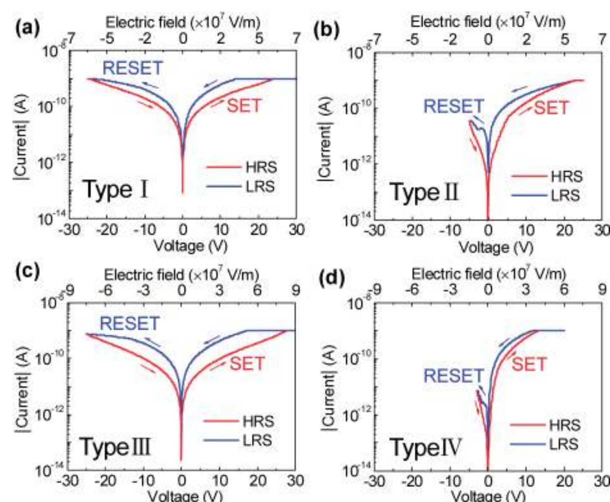

Figure 2. Typical $I-V$ curves of (a) Type I, (b) Type II, (c) Type III, and (d) Type IV junctions. High-resistance state (HRS) and low-resistance state (LRS) are highlighted by red and blue, respectively.

Table 1. Comparison between Four Junctions in the Ratio of SET and RESET Voltages (V_{SET}/V_{RESET})

junction type	V_{SET}/V_{RESET}
Type I	1.09
Type II	4.40
Type III	1.12
Type IV	4.01

the surroundings near the cathode seem to determine the occurrence and the characteristics of RS in NiO. It should be emphasized that obtaining such specific spatial information of RS is rather difficult for conventional capacitor-type RS devices because RS events occur at the inside space between metal electrodes in the case of the capacitor structures.

Here we discuss several critical issues in above experimental trends. First, there was a significant discrepancy between Types III and IV on their RS behaviors, in which the structural difference was solely the presence or the absence of the passivation layer for the entire region. When comparing the two RS behaviors, the symmetry of $I-V$ data was remarkably different, and the RESET voltage for Type IV was significantly lower than that of Type III. The critical role of surroundings on the bipolar RS behaviors of NiO nanowires has been identified by introducing various reactive gases in the surroundings.[6] In addition, for the bipolar RS of p-type NiO it has been reported that SET and RESET events correspond to oxidization and reduction, respectively.[6] Thus, the passivation layer must have such surrounding effects on the RS behaviors via altering the degree of redox events during RS operations. Therefore, the difference in the thermodynamic ground state due to the presence of passivation layer can cause the asymmetry of $I-V$ data via the stability of each resistance state (LRS or HRS), since the RS operation is the transition between the two states by an electric field. This remarkable surrounding effect on RS allows us to identify the spatial RS switching location, because we can intentionally introduce the surrounding effect at the limited spatial location by controlling the position of the passivation layer.

Next we question why the presence or the absence of the passivation layer near the cathode determines the characteristics of RS in NiO. The observed discrepancy between Types I and II junctions, which are partially passivated, indicates spatially inhomogeneous and asymmetric RS events. The similarity with Types III and/or IV junctions is also consistent with the scenario based on the spatially localized RS events. Thus, we should examine the reason why the spatially localized resistance change near the cathode occurs in the bipolar RS of NiO. On the basis of an electrochemical redox model and the p-type nature of NiO, the transition from HRS to LRS is related to "oxidization"; contrarily, the transition from LRS to HRS is related to "reduction". In the positive electric field of the present study, the transition from HRS to LRS always occurs, indicating that oxidization near the original cathode occurs via an oxygen ion migration with surroundings. On the other hand, in the negative electric field with the transition from LRS to HRS, a reduction occurs near the cathode. In n-type oxides such as TiO_2 and $SrTiO_3$, which have been intensively investigated for the RS applications,[11,12] an electrochemical model based on a redox event with an oxygen ion migration has most successfully explained many features of the bipolar RS behaviors.[12] The model describes the conduction paths comprising oxygen vacancies, which are formed by a migration of oxygen ions. Since negatively charged oxygen ions move toward the anode, the conduction paths comprising oxygen vacancies are formed from the cathode to the anode, creating the virtual cathode.[3] Thus, the bipolar RS in n-type oxides must occur near the anode.[13] This clearly differs from the present observation in NiO. In most n-type oxides, oxygen vacancies act as a donor, and the energy levels usually lie near the conduction band, giving mobile electrons via thermal excitation. However the scenario based on such conduction paths comprised of oxygen vacancies cannot apply to the bipolar RS of NiO because the energy level of oxygen vacancies in NiO is far from the conduction band.[14] Cation vacancies in NiO are well-known to give hole carriers via creating an acceptor level near the valence band[14] Previously we have demonstrated the p-type nature of mobile carriers responsible for the electrical conduction in the bipolar RS of NiO.[6] Here we consider the migration of oxygen ions because the diffusion of nickel ions has been reported to be 3 orders of magnitude faster than that of oxygen ions in NiO.[15] In addition, excess oxygen can create apparent cation vacancies in nonstoichiometric NiO.[16] On the basis of these experimental facts, we consider an electrochemical model via an ion migration and hole carriers to understand the bipolar RS of NiO. The model describes that negatively charged oxygen ions move toward the anode, creating apparent cation vacancies near the anode. This is consistent with implications of previous reports by utilizing conducting atomic force microscopy, which has revealed the movement and the crucial role of oxygen due to the electric field on the bipolar RS of NiO.[10] The resultant apparent cation vacancies due to the migration of oxygen ions create the conduction paths for hole carriers from the anode to the cathode, forming a virtual anode. This model in fact is an inverse analogue of an electrochemical model for n-type oxides[17] and can rigorously capture the occurrence of RS near the cathode rather than the anode for the bipolar RS in NiO.

In summary, we have successfully demonstrated the spatial switching location of bipolar RS in NiO by introducing asymmetrically passivated planar NiO nanowire junctions. We have identified that the bipolar RS in NiO occurs near the cathode rather than the anode. This trend can be interpreted in terms of an electrochemical model based on an ion migration and p-type conduction. Since the spatial information as to the bipolar RS in NiO cannot be extracted from capacitor-type RS devices due to the space limitation of structures, the present experimental approach would contribute further understanding of complex RS mechanisms and their chemical nature for various metal oxides.

■ ASSOCIATED CONTENT

Ⓢ Supporting Information. Detailed explanations as to fabrications, measurements and RS properties of devices; complete refs 2a,b. This material is available free of charge via the Internet at http://pubs.acs.org.

■ AUTHOR INFORMATION

Corresponding Author
yanagi32@sanken.osaka-u.ac.jp; kawai@sanken.osaka-u.ac.jp

■ ACKNOWLEDGMENT

This work was supported in part by NEXT Project. We thank T. Ishibashi for his invaluable technical support. T.K. and B.H.P. were partly supported by WCU program (Grant No. R31-2008-000-10057-0). T.K. was supported by FIRST.

■ REFERENCES

(1) (a) Strukov, D. B.; Snider, G. S.; Stewart, D. R.; Williams, R. S. *Nature* **2008**, *453*, 80. (b) Yang, J. J.; Pickett, M. D.; Stewart, D, R.; Li, X.; Ohlberg, A. A. D.; Stewart, D. R.; Williams, R. S. *Nat. Nanotechnol.* **2008**, *3*, 429. (c) Borghetti, J.; Snider, G. S.; Kuekes, P. J.; Yang, J. J.; Stewart, D. R.; Williams, R. S. *Nature* **2010**, *464*, 873.

(2) (a) Lee, M.; et al. *Adv. Funct. Mater.* **2008**, *18*, 1. (b) Ahn, S.; et al. *Adv. Mater.* **2008**, *20*, 924.

(3) (a) Linn, E.; Rosezin, R.; Kügeler, C.; Waser, R. *Nat. Mater.* **2010**, *9*, 403. (b) Waser, R.; Aono, M. *Nat. Mater.* **2007**, *6*, 833.

(4) (a) Waser, R.; Dittmann, R.; Staikov, G.; Szot, K. *Adv. Mater.* **2009**, *21*, 2632. (b) Kwon, D. H.; Kim, K. M.; Jang, J. H.; Jeon, J. M.; Lee, M. H.; Kim, G. H.; Li, X. S.; Park, G. S.; Lee, B.; Han, S. *Nat. Nanotechnol.* **2010**, *5*, 148.

(5) Oka, K.; Yanagida, T.; Nagashima, K.; Tanaka, H.; Kawai, T. *J. Am. Chem. Soc.* **2009**, *131*, 3434.

(6) Oka, K.; Yanagida, T.; Nagashima, K.; Kawai, T.; Kim, J. S.; Park, B. H. *J. Am. Chem. Soc.* **2010**, *132*, 6634.

(7) (a) Nagashima, K.; Yanagida, T.; Oka, K.; Taniguchi, M.; Kawai, T.; Kim, J. S.; Park, B. H. *Nano Lett.* **2010**, *10*, 1359. (b) Oka, K.; Yanagida, T.; Nagashima, K.; Tanaka, H.; Seki, S.; Honsho, Y.; Ishimaru, M.; Hirata, A.; Kawai, T. *Appl. Phys. Lett.* **2009**, *95*, 133110. (c) Nagashima, K.; Yanagida, T.; Tanaka, H.; Seki, S.; Saeki, A.; Tagawa, S.; Kawai, T. *J. Am. Chem. Soc.* **2008**, *130*, 5378–5382. (d) Marcu, A.; Yanagida, T.; Nagashima, K.; Oka, K.; Tanaka, H.; Kawai, T. *Appl. Phys. Lett.* **2008**, *92*, 173119. (e) Nagashima, K.; Yanagida, T.; Tanaka, H.; Kawai, T. *Appl. Phys. Lett.* **2007**, *90*, 233103. (f) Nagashima, K.; Yanagida, T.; Tanaka, H.; Kawai, T. *J. Appl. Phys.* **2007**, *101*, 124304. (g) Nagashima, K.; Yanagida, T.; Oka, K.; Kanai, M.; Klamchuen, A.; Kim, J. S.; Park, B. H.; Kawai, T. *Nano Lett.* **2011**, *11*, 2114.

(8) (a) Marcu, A.; Yanagida, T.; Nagashima, K.; Tanaka, H.; Kawai, T. *J. Appl. Phys.* **2007**, *102*, 016102. (b) Yanagida, T.; Nagashima, K.; Tanaka, H.; Kawai, T. *Appl. Phys. Lett.* **2007**, *91*, 061502. (c) Yanagida, T.; Nagashima, K.; Tanaka, H.; Kawai, T. *J. Appl. Phys.* **2008**, *104*, 016101. (d) Nagashima, K.; Yanagida, T.; Oka, K.; Tanaka, H.; Kawai, T. *Appl. Phys. Lett.* **2008**, *93*, 153103. (e) Yanagida, T.; Marcu, A.; Matsui, H.; Nagashima, K.; Oka, K.; Yokota, K.; Taniguchi, M.; Kawai, T. *J. Phys. Chem. C* **2008**, *112*, 18923. (f) Nagashima, K.; Yanagida, T.;

Klamchuen, A.; Kanai, M.; Oka, K.; Seki, S.; Kawai, T. *Appl. Phys. Lett.* **2010**, *96*, 073110.

(9) (a) Herderick, E. D.; Reddy, K. M.; Sample, R. N.; Draskovic, T. I.; Padture, N. P. *Appl. Phys. Lett.* **2009**, *95*, 203505. (b) Choi, J. S.; Kim, J. S.; Hwang, I. R.; Hong, S. H.; Jeon, S. H.; Kang, S. O.; Park, B. H.; Kim, D. C.; Lee, M. J.; Seo, S. *Appl. Phys. Lett.* **2009**, *95*, 022109.

(10) (a) Yoshida, C.; Kinoshita, K.; Yamasaki, T.; Sugiyama, Y. *Appl. Phys. Lett.* **2008**, *93*, 042106. (b) Lee, M. H.; Song, S. J.; Kim, K. M.; Kim, G. H.; Seok, J. Y.; Yoon, J. H.; Hwang, C. S. *Appl. Phys. Lett.* **2010**, *97*, 062909. (c) Kinoshita, K.; Okutani, T.; Tanaka, H.; Hinoki, T.; Yazawa, K.; Ohmi, K.; Kishida, S. *Appl. Phys. Lett.* **2010**, *96*, 143505.

(11) (a) Shin, J.; Kim, I.; Biju, K. P.; Jo, M.; Park, J.; Lee, J.; Jung, S.; Lee, W.; Kim, S.; Park, S.; Hwang, H. *J. Appl. Phys.* **2011**, *109*, 033712. (b) Xia, Q.; Yang, J. J.; Wu, W.; Li, X.; Williams, R. S. *Nano Lett.* **2010**, *10*, 2909. (c) Kügeler, C.; Zhang, J.; Hoffmann-Eifert, S.; Kim, S. K.; Waser, R. *J. Vac. Sci. Technol., B* **2011**, *29*, 01AD01-1.

(12) Szot, K.; Speier, W.; Bihlmayer, G.; Waser, R. *Nat. Mater.* **2006**, *5*, 312.

(13) (a) Jeong, D. S.; Schroeder, H.; Breuer, U.; Waser, R. *J. Appl. Phys.* **2008**, *104*, 123716. (b) Jeong, D. S.; Schroeder, H.; Waser, R. *Phys. Rev. B* **2009**, *79*, 195317. (c) Biju, K. P.; Liu, X.; Bourim, E. M.; Kim, I.; Jung, S.; Pak, J.; Hwang, H. *Electrochem. Solid-State Lett.* **2010**, *13*, H443.

(14) (a) Park, S.; Ahn, H. S.; Lee, C. K.; Kim, H.; Jin, H.; Lee, H. S.; Seo, S.; Yu, J.; Han, S. *Phys. Rev. B* **2008**, *77*, 134103. (b) Lee, H. D.; Magyari-Köpe, B.; Nishi, Y. *Phys. Rev. B* **2010**, *81*, 193202.

(15) (a) Volpe, M. L.; Reddy, J. *J. Chem. Phys.* **1970**, *53*, 1117. (b) Dubois, C.; Monty, C.; Philibert, J. *Philos. Mag. A* **1982**, *46*, 419.

(16) (a) Aiken, J. G.; Jordan, A. G. *J. Phys. Chem. Solids* **1968**, *29*, 2153. (b) Mitof, S. P. *J. Chem. Phys.* **1961**, *35*, 882. (c) Osburn, C. M.; Vest, R. W. *J. Phys. Chem. Solids* **1971**, *32*, 1331.

(17) Cho, E.; Han, S.; Ahn, H. S.; Lee, K. R.; Kim, S. K.; Hwang, C. S. *Phys. Rev. B* **2006**, *73*, 193202.